

# Red Antenna States of Photosystem I from Cyanobacteria *Synechocystis* PCC 6803 and *Thermosynechococcus elongatus*: Single-Complex Spectroscopy and Spectral Hole-Burning Study

Kerry J. Riley,<sup>†</sup> Tõnu Reinot,<sup>†</sup> Ryszard Jankowiak,<sup>\*,‡</sup> Petra Fromme,<sup>§</sup> and Valter Zazubovich<sup>\*,||</sup>

Department of Chemistry, Iowa State University, Ames, Iowa 50011; Department of Chemistry, Kansas State University, Manhattan, Kansas 66506; Department of Chemistry and Biochemistry, Arizona State University, Tempe, Arizona 85287; and Department of Physics, Concordia University, 7141 Sherbrooke Street West, Montreal, Quebec H4B1R6, Canada

Received: May 1, 2006; In Final Form: September 14, 2006

Hole-burning and single photosynthetic complex spectroscopy were used to study the excitonic structure and excitation energy-transfer processes of cyanobacterial trimeric Photosystem I (PS I) complexes from *Synechocystis* PCC 6803 and *Thermosynechococcus elongatus* at low temperatures. It was shown that individual PS I complexes of *Synechocystis* PCC 6803 (which have two red antenna states, i.e., C706 and C714) reveal only a broad structureless fluorescence band with a maximum near 720 nm, indicating strong electron–phonon coupling for the lowest energy C714 red state. The absence of zero-phonon lines (ZPLs) belonging to the C706 red state in the emission spectra of individual PS I complexes from *Synechocystis* PCC 6803 suggests that the C706 and C714 red antenna states of *Synechocystis* PCC 6803 are connected by efficient energy transfer with a characteristic transfer time of  $\sim 5$  ps. This finding is in agreement with spectral hole-burning data obtained for bulk samples of *Synechocystis* PCC 6803. The importance of comparing the results of ensemble (spectral hole burning) and single-complex measurements was demonstrated. The presence of narrow ZPLs near 710 nm in addition to the broad fluorescence band at  $\sim 730$  nm in *Thermosynechococcus elongatus* (Jelezko et al. *J. Phys. Chem. B* 2000, 104, 8093–8096) has been confirmed. We also demonstrate that high-quality samples obtained by dissolving crystals of PS I of *Thermosynechococcus elongatus* exhibit stronger absorption in the red antenna region than any samples studied so far by us and other groups.

## Introduction

Photosystem I (PS I) is one of the two major photosystems involved in oxygenic photosynthesis and the largest, most complex membrane protein for which detailed structural and functional information is available.<sup>1,2</sup> PS I converts light energy into chemical energy by transferring electrons across the thylakoid membrane from plastocyanine or cytochrome *c*<sub>6</sub> to ferredoxin. Structures of PS I from the cyanobacterium *Thermosynechococcus elongatus*<sup>2</sup> (formerly *Synechococcus elongatus*; we will use *Synechococcus* as a shorthand in the following discussion) and higher plant *Pisum sativum*<sup>3</sup> were recently determined at 2.5 and 4.4 Å resolution by X-ray crystallography. A recent computational study provided an atomic model of plant PS I.<sup>4</sup> While cyanobacterial PS I is trimeric,<sup>2</sup> that of higher plants is monomeric with the core surrounded by peripheral antenna complexes.<sup>3,4</sup> (PS I of the deep-water, low-illumination strains of cyanobacterium *Prochlorococcus marinus*<sup>5</sup> as well as some other cyanobacteria grown under iron stress conditions<sup>6,7</sup> also contains peripheral light-harvesting complexes, the *IsiA* and *PcB* proteins that form a ring surrounding the trimeric PS I core.) The similarity of the core structures of PS I from cyanobacteria

and plants indicates that evolution caused only minor variations in the core organization and function and also provides a legitimate reason to believe that the structure and function of PS I cores from other organisms are also similar. Each core monomer is a complex network of chlorophyll *a* (Chl *a*) molecules embedded in protein with  $\sim 90$  antenna Chls *a* surrounding the “reaction center” (containing the electron-transfer chain which consists of primary electron-donor P700, accessory Chls *a*, phylloquinone, and three 4Fe4S clusters) and funneling sunlight energy into it. While the majority of antenna Chls *a* absorb at 670–690 nm, some absorb at even longer wavelengths than the strongly coupled reaction center dimer, P700.<sup>8,9</sup> It has been shown that these “red antenna states” are localized on multimers of Chls *a* (closely spaced and strongly coupled) rather than on single Chl *a* molecules that interact peculiarly with their protein environment. Three red antenna states (C710, C715, C719) were resolved in PS I of *Synechococcus*<sup>10</sup> and two (C706 and C714) in PS I of *Synechocystis* PCC 6803.<sup>9,11</sup> Spectral hole-burning (SHB) experiments<sup>9,10,12</sup> showed that several properties of the lowest energy antenna states of *Synechococcus* (C719) and *Synechocystis* (C714) PS I are nearly identical, suggesting that same chlorophyll ensembles are responsible for those red antenna states, with the small difference in their energy most likely due to small differences in protein environment. Both states revealed strong electron–phonon coupling, large permanent dipole moment change, and large rates of pressure-induced shift of spectral holes (lines)

\* To whom correspondence should be addressed. E-mail: (R.J.) ryszard@ksu.edu and (V.Z.) vzazubov@alcor.concordia.ca..

<sup>†</sup> Iowa State University.

<sup>‡</sup> Kansas State University.

<sup>§</sup> Arizona State University.

<sup>||</sup> Concordia University.

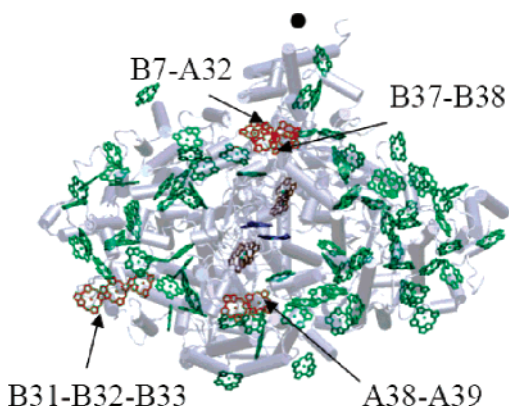


**Figure 1.** Chlorophyll ensembles proposed to be the origin of the red antenna states in PS I of *Synechococcus* in ref 13. (Figure 1 from ref 14, depicting PS I monomer, was used as a template.) Black dot indicates the approximate location of the symmetry axis of the PS I trimer.

indicating that electron-exchange interaction contributes significantly to the excitonic coupling of the lowest energy C714 and C719 ensembles. The relations between structural and spectral features in cyanobacterial PS I remain undetermined. Originally, based on the strength of the dipole–dipole coupling between the chlorophyll molecules, B31–B32–B33, A38–A39, B37–B38, and B7–A32 were identified as the most probable origins of the red antenna states in *Thermosynechococcus elongatus*<sup>13</sup> (Figure 1). The structure of PS I from *Synechocystis* was not measured; however, taking into account the similarity between the structures of *Synechococcus*<sup>2</sup> and plant<sup>3</sup> PS I, one might expect that the PS I structure for *Synechosystis* is quite similar to that for *Synechococcus*. For interpigment distances smaller than 10 Å the use of dipole–dipole approximation is questionable. On the basis of the results of full Coulomb<sup>14</sup> and INDO/S calculations,<sup>15</sup> respectively, several other chlorophyll dimers were identified which could contribute to the PS I absorption at  $\lambda > 700$  nm, namely, A33–A34, A24–A35, and B22–B34<sup>14</sup> or A33–A34, A26–A27, A10–A18, A12–A14, B09–B17, and B24–B25.<sup>15</sup> Note that both refs 14 and 15 still predict strong coupling between chlorophylls involved in the B07–A32 dimer (or B06–B07–A31–A32 tetramer) as well as for the A38–A39 and B37–B38 dimers but not for the B31–B32–B33 trimer. Balaban suggested that the *syn*-ligated chlorophyll dimers B02–B03 and A03–A04 are responsible for the red antenna states in cyanobacterial PS I.<sup>16,17</sup> Gobets et al. concluded from fluorescence kinetics data that the lowest energy red antenna state is localized on the B31–B32–B33 trimer in the PS I of *Synechococcus*.<sup>18</sup> This assignment, however, contradicts the spectral hole-burning results demonstrating the similarity between the C714 state of *Synechocystis* and the C719 state of *Synechococcus*.<sup>9,10,12</sup> (Note that the B31–B32–B33 trimer most probably is absent or at least rearranged/disrupted in *Synechocystis* due to the lack of the histidine residue coordinating the respective chlorophylls of *Synechococcus*.)<sup>14,18</sup> In addition, assignment of the *Synechococcus* red antenna states to the B31–B32–B33 trimer is inconsistent with data<sup>8,9</sup> indicating that the lowest energy red states of both *Synechococcus* (C719) and *Synechocystis* (C714) are localized close to the trimerization domain of PS I.

SHB is a powerful frequency domain technique for studying the  $S_1(Q_y)$  excited-state electronic structure, excitation energy transfer (EET), and electron-transfer (ET) dynamics of protein–chlorophyll complexes at low temperatures. Despite its frequency selectivity, SHB still probes inhomogeneous ensembles

of complexes, meaning that certain properties may be subject to distribution for chlorophylls absorbing at the same wavelength. This is manifested, for example, by broadening of the spectral holes in external pressure and electric fields.<sup>19</sup> Single photosynthetic complex spectroscopy allows the properties of the complexes to be individually investigated, thereby removing effects due to inhomogeneity. While significant progress has been achieved in the spectroscopic studies of single LH-2 complexes<sup>20–26</sup> as well as LH-1<sup>27,28</sup> and LHC-II<sup>29</sup> complexes, there is very little single-complex data available for PS I. Until recently, there has been only one paper published on single PS I from *Thermosynechococcus elongatus*<sup>30</sup> (the data from this paper was later included in several reviews). The main feature of the individual PS I spectra in ref 30 was a broad structureless band peaked at about 725–730 nm. This band was accompanied by several narrow lines at 710–712 nm. The former broad band has been assigned to the same state which exhibited very strong electron–phonon coupling in SHB experiments.<sup>10</sup> The same group published another paper on single PS I earlier this year.<sup>31</sup> It was demonstrated that the emission of prerduced PS I is multicomponent, since after intensive ( $\sim 600 \mu\text{W}$ ) illumination resulting in bleaching of the main fluorescence band peaked at  $\sim 730$  nm, a second emission component, peaked at 745 nm became observable. It was not determined, though, which absorption band corresponds to the emission band at  $\sim 745$  nm. Undoubtedly, the lack of published results is due to the complexity of PS I. As mentioned above, there are 288 Chls *a* per PS I trimer, i.e., almost 300 spectral lines/bands in a relatively narrow wavelength range. Furthermore, PS I does not possess the high symmetry of the light-harvesting complexes from purple bacteria,<sup>20–28</sup> which reduces the number of observable lines in the spectra of those complexes. Jelezko et al. focused exclusively on the red antenna state region of PS I from *Synechococcus*. As mentioned above, their results confirmed that the lowest energy state (C719) is characterized by very strong electron–phonon coupling.<sup>30</sup> On the other hand, their observation of narrow zero-phonon lines near 711–712 nm, most likely belonging to the higher energy red state(s) of *Synechococcus*, present in both emission and fluorescence excitation spectra, suggested that different red antenna states (i.e., C710 and C719) are not connected by efficient energy transfer at low temperatures. This suggestion, however, contradicts the fluorescence anisotropy data,<sup>8</sup> which indicates that C710  $\rightarrow$  C719 energy transfer in *Synechococcus* does occur. To address the nature of the red antenna absorption bands, energy transfer, and the low-energy emitting states, we describe below SHB results obtained for bulk PS I samples and the single-complex emission spectra of PS I from both *Thermosynechococcus elongatus* and *Synechocystis* PCC 6803 obtained under identical experimental conditions. We will also demonstrate the importance of comparing the results of conventional absorption and emission spectroscopy (ensemble, low resolution), spectral hole-burning (ensemble, high resolution), and single-complex spectroscopy, which has rarely been done in the same manuscript.

## Experimental Methods

Wild-type trimeric PS I complexes from *Synechocystis* PCC 6803 were extracted as described in ref 9. The concentrated samples (stored at  $-70^\circ\text{C}$ ) were from the same batch as those used in our earlier hole-burning experiments.<sup>9,12</sup> Wild-type trimeric PS I complexes from *Thermosynechococcus elongatus* were prepared by dissolving high-quality crystals similar to those used in X-ray diffraction experiments<sup>2</sup> in buffer containing 5 mM Mes, pH 6.4, 50 mM  $\text{MgSO}_4$ , and 0.02% dodecylmaltoside.

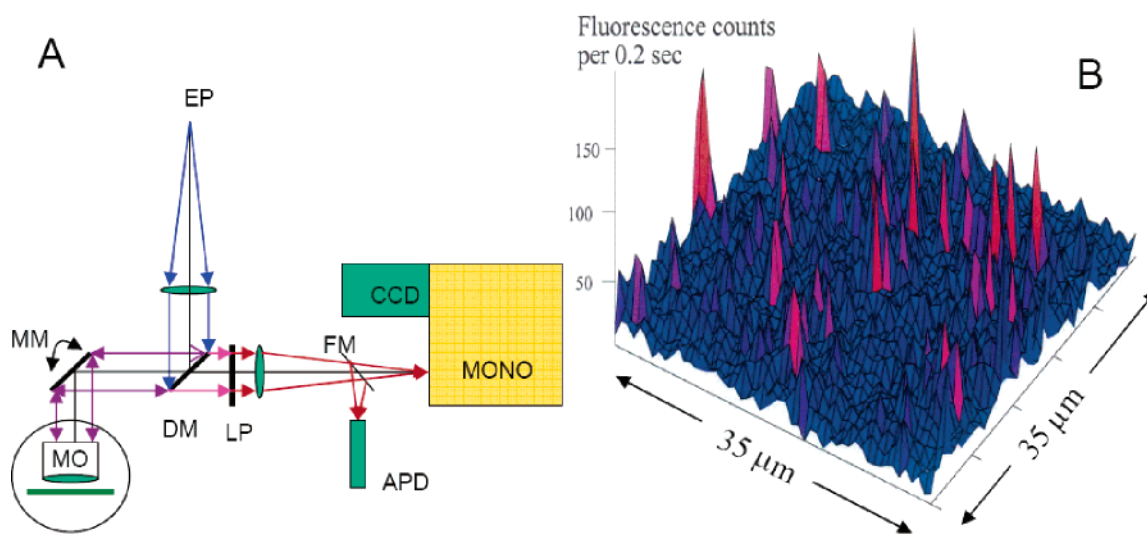


**Figure 2.** (A) Scheme of the confocal microscope used for individual complex spectroscopy. EP is excitation pinhole, DM is dichroic mirror, MM is motorized mirror, MO is microscope objective, LP is long-pass filter, and FM is flipping mirror. APD itself and the monochromator's slit were used as detection pinholes. (B) Raster-scan image of the thin film containing single PS I complexes from *Synechocystis* PCC 6803 (red peaks) obtained by varying the orientation of the scanning mirror. Fluorescence was collected with a 180  $\mu\text{m}$ -diameter avalanche photodiode used as a pinhole. Complexes were excited with 250  $\text{nW}/\mu\text{m}^2$  (25  $\text{W}/\text{cm}^2$ ) at 680 nm, and fluorescence was collected at  $\lambda > 700$  nm.  $T = 10$  K.

For bulk experiments, the above solution was mixed with buffer (10 mM MOPS, 0.02%  $\beta$ -dodecylmaltoside, pH = 7) and then mixed with glycerol (1:2), so that the final Chl *a* concentration was  $\sim 2 \times 10^{-5}$  M. The buffer–glycerol matrix provides good-quality glass upon cooling to liquid helium temperatures. Absorption spectra and hole-burning spectra were measured with a Bruker IFS 120HR Fourier-transform spectrometer at 2  $\text{cm}^{-1}$  resolution. Spectral holes were burned with a Coherent CR-699 laser with Exciton LD-688 dye (650–720 nm). Bulk emission spectra were measured with  $\sim 1$  nm resolution using a McPherson 2061 1-m focal length monochromator with a Princeton Instruments diode array as a detector. These spectra were obtained with an excitation wavelength of 308 and/or 514 nm.

For experiments involving single complexes, concentrated PS I samples were first diluted with a suitable buffer (vide supra) to achieve the  $\text{OD}_{680} \approx 0.4$  per 1 cm thickness, which corresponds to a Chl *a* concentration of approximately  $10^{-5}$  M, i.e., to a concentration of trimeric PS I complexes of less than  $10^{-7}$  M, taking into account 96 Chl *a* per P700. This solution was diluted again in a buffer/glycerol mixture (3:1) by a factor of  $\sim 1000$  and then spin-coated on a plasma-cleaned sapphire plate yielding a film thickness of less than 1  $\mu\text{m}$ . Use of glycerol here was not meant to facilitate formation of a transparent glass but to adjust the viscosity of the solution for better thin film formation. Polymers were not used for sample preparation because, based on our experience (unpublished results), the photosynthetic complexes embedded in dry polymer films are disrupted compared to those studied in typical bulk experiments. The sample was placed in a cold ( $< 0^\circ\text{C}$ ), dark, oxygen-free cryostat, and temperature was lowered to liquid helium temperature in about 20 min. Experiments were performed at 10 K in helium gas or at 2 K in superfluid helium. To avoid sample degradation, all room-temperature sample-handling procedures were performed in dim light as quickly as possible.

The optical setup was based on a home-built confocal microscope with a Newport 60  $\times$  0.85 NA achromatic objective attached to the sample holder inside the cryostat (Janis). In order to reduce sample movements due to temperature expansion, the rod of the sample holder was made from fused quartz. The sample was moved in relation to the objective along the

objective axis using an electromagnet with two parallel coils, one superconducting (for  $T < 7\text{K}$ ) and the other made from copper wire. A computer-controlled scanning mirror was used to move the focal spot across the sample plane. Excitation was performed with a Coherent CR-699 laser with Exciton LD-688 dye (650–720 nm) and with intracavity etalons removed, providing a line width of several GHz. After adjustment to ensure that the PS I-containing film was indeed in the focal plane of the objective, the scanning mirror was moved while the fluorescence (excited at 675–680 nm) was collected (at  $\lambda > 700$  nm) by the avalanche photodiode (Perkin-Elmer, dark count  $< 25\text{ s}^{-1}$ ). The experimental setup is schematically depicted in Figure 2A. An example of the resulting 10 K “raster-scan” image is presented in Figure 2B. The fluorescence peaks (red) correspond to individual PS I complexes from *Synechocystis* PCC 6803. In order to focus on individual complexes, the mirror was then moved to positions determined from the raster-scan image and spectroscopic measurements were performed. Emission spectra were collected with either a Princeton Instruments PI-MAX intensified CCD camera or a liquid-nitrogen-cooled, back-illuminated CCD camera through an Omega AELP 700 long-pass filter (and DRLP 710 dichroic mirror) and a Jobin-Yvon Triax 320 spectrometer with a resolution of 0.4 nm. Excitation was at 675–680 nm. Excitation intensities (adjusted using neutral filters, LOMO) are given in the figure captions. In calculating these intensities it was assumed that the laser was focused at a 1  $\mu\text{m}^2$  spot. In order to reduce background (mainly broadband dye fluorescence) an Omega Third Millennium SP700 short-pass filter was placed after the laser power stabilizer (BEOC).

## Results and Discussion

***Synechocystis* PCC 6803.** The bulk 5 K emission spectrum of trimeric PS I from *Synechocystis* PCC 6803 showed a single fluorescence origin band with a maximum near 720 nm (see below), in agreement with emission spectra reported in refs 9 and 33. The shapes of the absorption spectrum and satellite hole structure resulting from downhill excitation energy transfer following high-energy excitation were also in agreement with earlier results.<sup>9,12</sup> Therefore, it is assumed in the following



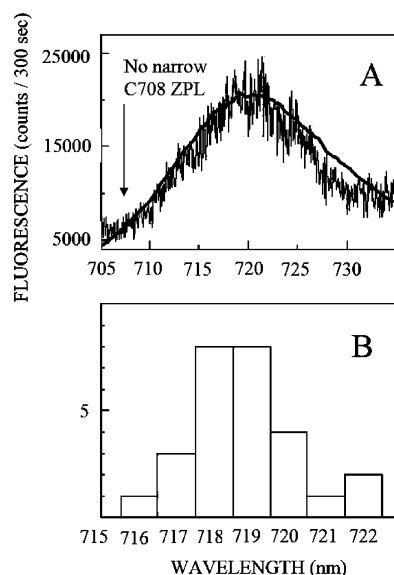


**Figure 3.** (A) Typical emission spectrum of a single PS I complex from *Synechocystis* PCC 6803 excited at 675 nm. Approximately 1.5  $\mu\text{W}$  was focused on the single complex (i.e., the excitation intensity was  $\sim 150 \text{ W/cm}^2$  assuming  $1 \mu\text{m}^2$  focal area), and the collection time was 300 s.  $T = 10 \text{ K}$ . Bulk emission spectrum (thick solid curve; excitation at 308 nm) is superimposed on the single-complex emission spectrum. (B) Histogram of the emission band maximum wavelengths based on the data from 27 single PS I complexes. Excitation was at 675 nm.

discussion that the spectra described reflect the properties of the intact trimeric *Synechocystis* PS I complexes.

The noisy spectrum in Figure 3A is a typical low-temperature emission spectrum of a single PS I complex from *Synechocystis* PCC 6803. The spectrum peaks at 720 nm and is quite broad (fwhm=12 nm) and structureless. This result is in agreement with the spectral hole-burning data<sup>9,37</sup> and supports the assignment of ref 9 where it was demonstrated that electron–phonon coupling for the emitting (C714) state is very strong, with a total Huang–Rhys factor  $S$  of about 2. The strong electron–phonon coupling, along with possible light-induced spectral diffusion, is the reason why ZPLs belonging to the C714 state were not observed. Similar strong electron–phonon coupling for the lowest energy red antenna state of single PS I complexes from *Synechococcus* (C719) was demonstrated in ref 30. No sharp zero-phonon lines were observed near 706–708 nm, where direct emission from the C706 state might be expected. At this point, it may be asked if this finding actually suggests that there is only one red antenna state in *Synechocystis* PCC 6803, as proposed in ref 18. However, as demonstrated in refs 9 and 34, electron–phonon coupling changes across the red antenna absorption band, becoming significantly weaker at 706–710 nm ( $S \leq 1.2$ ) than at 714–718 nm ( $S \approx 2$ ). Furthermore, significant differences were also observed for the permanent dipole moment change between excited- and ground-state  $\Delta\mu$ ,<sup>9</sup> again supporting the presence of more than one red antenna state. We are unaware of a theoretical model that could explain the variation of  $S$  and  $\Delta\mu$  by a factor of 2 within a single inhomogeneously broadened band. However, let us assume for a moment that just one red antenna state with such correlation is present in PS I and consider its possible manifestations on a single-complex level. The emission from the PS I complexes with the one and only lowest state absorption at longer wavelengths (for example at  $\sim 715 \text{ nm}$ ) is expected at  $\sim 720 \text{ nm}$  and should be broad and structureless due to strong electron–phonon coupling,  $S \approx 2$  (as observed). The emission

from PS I complexes with the lowest state absorbing at shorter wavelength (for example at  $\sim 708 \text{ nm}$ ) is expected to contain a well-defined ZPL at about the same wavelength (due to weaker electron–phonon coupling,  $S \leq 1.2$ ). The single-complex spectroscopy results in Figure 3B definitely do not fit this line of reasoning. Figure 3B contains the diagram of the emission band maxima of 27 single complexes. All measured single-complex emission spectra contained only a broad band peaked at 716–722 nm; none exhibited narrow zero-phonon lines at  $\sim 708 \text{ nm}$ . Also, the bulk emission spectra in this work and in refs 9 and 33 did not exhibit any shoulders at 706–710 nm. (For easy comparison, the bulk emission spectrum of *Synechocystis* PS I is superimposed on the single-complex spectrum in Figure 3A.) This is a good illustration of the importance of comparing the results of single-complex spectroscopy with those of ensemble techniques, such as SHB, whenever possible. The results of single-complex spectroscopy alone do not prove that there are two red antenna states in PS I of *Synechocystis* PCC 6803. Likewise, the SHB results alone do not allow distinguishing between the cases of two red antenna states and of one state with a correlation between the wavelength and the electron–phonon coupling. Only when the two techniques are combined do the results prove the presence of the two states.

The absence of narrow lines in the spectra of single PS I from *Synechocystis* PCC 6803 may indicate that the red antenna states in *Synechocystis* are connected by fast and efficient energy transfer, in agreement with spectral hole-burning results<sup>12</sup> which yield 5–6 ps for the C706 state lifetime. (Obviously, a 5–6 ps energy-transfer time corresponds to a quite narrow,  $\sim 1 \text{ cm}^{-1}$ , ZPL. Since the fluorescence lifetime of the C706 state is in the nanosecond range, the fluorescence yield must be smaller than 0.005, which makes ZPL unobservable in single-complex experiments at 0.4 nm resolution, especially if spectral diffusion is present.) However, to prove that we were capable to observe narrow ZPLs using our experimental setup, single PS I complexes from *Thermosynechococcus elongatus* were also studied and results compared to those described in refs 30 and 31.

***Thermosynechococcus elongatus.*** Unlike in previous spectroscopic studies, here the *Thermosynechococcus elongatus* PS I samples were prepared by dissolving high-quality PS I crystals. Absorption and hole-burning spectra of trimeric PS I from *Synechococcus* are presented in Figure 4 along with the absorption spectrum obtained earlier for conventionally prepared sample under similar conditions.<sup>10</sup> The absorption spectra are normalized for equal bulk antenna absorption at  $\sim 680 \text{ nm}$ . The absorption spectrum (thick solid curve in A) is similar to that reported in refs 8, 10, and 32 except for the red antenna state region ( $\sim 700$ – $740 \text{ nm}$ ), which appears to have significantly greater oscillator strength. In addition, a comparison of the shapes of the absorption spectra in the 700–740 nm region suggests that the relative intensity of the band peaking at 710 nm is approximately the same for both samples while the intensities of the lower energy (C715 and C719) bands are greater for the sample studied in this work. To test this suggestion, we explored the shape of the hole spectra (and its time evolution during the hole-burning process) resulting from nonresonant excitation at 670 nm (Figure 4B). Formation of satellite holes at lower energies is due to downhill energy transfer followed by spectral hole burning. At low burn fluences ( $\leq 10 \text{ J/cm}^2$ ) the only low-energy satellite hole observed is peaked at 719 nm (dotted curve in Figure 4B). In our experiment, the hole at 719 nm was observable directly, in contrast to the spectra presented in ref 10, where the C719 state

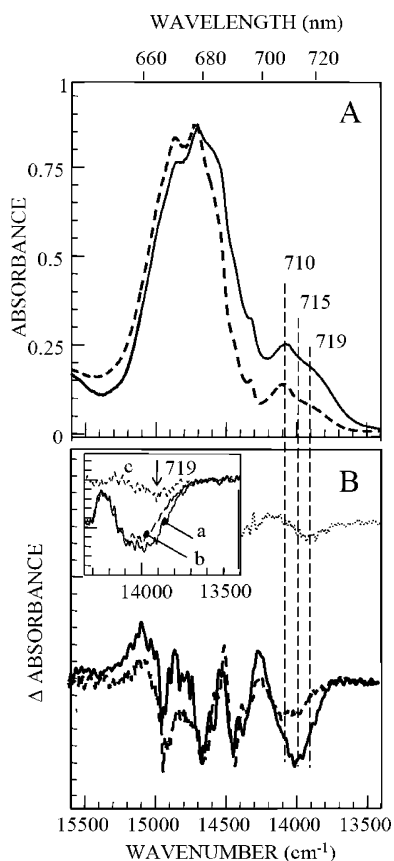


**Figure 4.** Five Kelvin bulk spectra of PS I of *Thermosynechococcus elongatus*. (A) Bulk absorption spectra: (thick solid curve) Trimeric PS I sample used in this work; (thick dashed curve) trimeric PS I sample used in.<sup>10</sup> Spectra are normalized to approximately equal absorbance in the bulk antenna region,  $\sim 680$  nm. (B) Satellite hole spectra resulting from illumination at 670 nm of the trimeric PS I sample used in this work with about 10 (25 mW/cm<sup>2</sup> for 420 s; dotted curve) and about 500 J/cm<sup>2</sup> (several burns with intensity of up to 300 mW/cm<sup>2</sup>; solid curve). (thick dashed curve) Hole spectrum resulting from illumination at 670 nm with about 500 J/cm<sup>2</sup> for the sample explored in ref 10. (Insert) Evolution of the hole spectrum shape for the sample described in ref 10. Solid curve a corresponds to a burning fluence of about 3 J/cm<sup>2</sup> and long-dashed curve b to about 100 J/cm<sup>2</sup>. Curve a was multiplied by a factor of  $\sim 2$  to normalize it to curve b at 700 nm (14 285 cm<sup>-1</sup>). Short-dashed curve c is the difference of curves a and b.

was only detectable in the difference (curve c in the insert in Figure 4B) of satellite hole spectra obtained with different burn fluences (curves a and b in the insert in Figure 4B). With the increase of the burning dose, the 719 nm hole became obscured by the much stronger hole peaked at 715 nm. Thick solid and dashed curves in Figure 4B are hole spectra resulting from irradiation with 500 J/cm<sup>2</sup> at 670 nm for samples studied in this work and in ref 10, respectively. In earlier work the third satellite hole, at 710 nm, was as strong as the 715 nm hole.<sup>10</sup> However, in this work (solid curve in Figure 4B), the 710 nm hole is just a shoulder compared to the 715 nm hole. Thus, we conclude that C715 and C719 bands in our samples have higher oscillator strengths than in other *Thermosynechococcus elongatus* PS I samples explored thus far. Note that the integral intensity and shape of the red antenna region are sensitive to the monomeric/trimeric state of PS I. Such a tendency was observed for both *Synechococcus*<sup>8</sup> and *Synechocystis*.<sup>9</sup> Therefore, one might conclude that the supposedly trimeric *Synechococcus* samples in the previous studies by us and other groups could, in fact, contain a certain fraction of monomeric PS I. The emission spectrum (Figure 5, solid curve) is peaked at 732

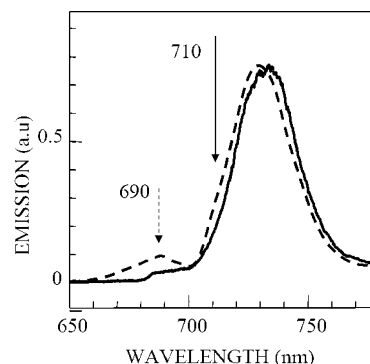


**Figure 5.** Five Kelvin emission spectra (excited at 308 nm) of the *Synechococcus* PS I samples used in this work (solid curve) and in ref 10 (dashed curve). Spectra are normalized to equal intensity at 730–732 nm. Solid arrow indicates the shoulder at 710 nm in the spectrum from ref 10. Dashed arrow indicates a feature at  $\sim 690$  nm.

nm, at approximately the same wavelength as in the previously described samples (dashed curve in Figure 5; from ref 10). This emission band is assigned to the same chlorophylls which have their absorption maximum at 719 nm (C719), in agreement with the data on electron–phonon coupling.<sup>10</sup> In this work, no weak shoulders near 710 nm (indicated by the solid arrow) were observed. Also, the band at  $\sim 685$ – $690$  nm (indicated by the dashed arrow) was significantly weaker than in earlier works. No contribution from disconnected chlorophylls, which might be expected at  $\sim 670$  nm, could be detected. Resonant hole-burning experiments (results not shown) confirmed that the electron–phonon coupling is very strong ( $S \geq 2$ ) for the C719 state and relatively weak ( $S \approx 1$ ) for the C710 state, in agreement with earlier work.<sup>10</sup> Thus, we concluded that the *Synechococcus* samples appear to be the most intact trimeric PS I samples studied thus far.

The emission spectra of individual PS I complexes from *Thermosynechococcus elongatus* are shown in Figure 6. The main feature of the individual PS I spectra is a broad band peaked at about 725–727 nm, in good agreement with ref 30. This band closely resembles the bulk emission spectrum and most likely originates from the C719 state, characterized by strong electron–phonon coupling.<sup>10</sup> This broad band was sometimes accompanied by narrow lines at 706–713 nm. Assuming weak to moderate electron–phonon coupling observed with SHB at  $\sim 710$  nm,<sup>10</sup> the absorption maximum of the state from which the narrow ZPLs originate should be 709–710 nm in the bulk spectra, i.e., the lines most likely belong to the C710 state. Narrow zero-phonon lines (ZPL) in the 706–713 nm region were at least occasionally observed in 80% of the single complexes. The relative intensities of these narrow ZPL and of the main emission band at  $\sim 725$ – $727$  nm varied from one complex to another. The number of lines also varied from one complex to another and from spectrum to spectrum for the same complex, so that no lines were observed in about 50% of the spectra. Figure 6A–C shows consecutively collected emission spectra of three different complexes. (Periodic features at  $\lambda > 730$  nm most probably originate from the etaloning effect of the back-illuminated CCD, i.e., the interference between reflections from the front and back surfaces of a thinned back-illuminated CCD chip.) It is evident that the positions of the sharp lines varied with time, and sometimes the lines disappeared entirely only to reappear later (on the time scale of tens of seconds). This is an indication of relatively slow spectral diffusion. For fixed laser excitation intensity, we did not notice any significant statistical difference between either the probability of observing narrow lines or their spectral diffusion

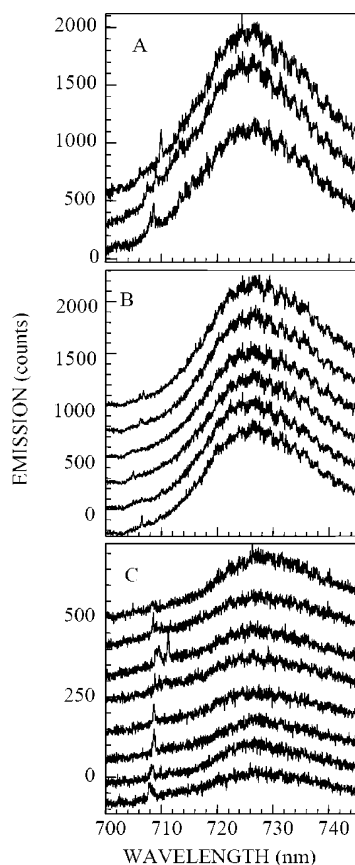


**Figure 6.** Single-complex emission spectra of PS I of *Thermosynechococcus elongatus*. About  $5 \mu\text{W}$  at  $680 \text{ nm}$  was focused to a spot of about  $1 \mu\text{m}^2$  (i.e., the excitation intensity was  $500 \text{ W/cm}^2$ ), and collection times were 300 (A) and 60 s (B and C). A–C contain spectra of three different complexes. Consecutively taken spectra of the same complex are depicted in each frame.  $T = 9 \text{ K}$ . Spectra are shifted along the vertical axis for clarity.

behavior at 10 and 2 K. (Unfortunately, we were unable to follow the same single complex from 10 to 2 K.) Thus, we conclude that the observed spectral diffusion is predominantly light-induced and not thermally-induced. In other words, we observed a process analogous to nonresonant spectral hole burning in the bulk experiments (Figure 4B). The relative insignificance of thermally-induced spectral diffusion is consistent with the slow filling of spectral holes below 20 K in the dark.

Single-complex emission spectra obtained for PS I in this work as well as in work previously published by Jelezko et al.<sup>30</sup> indicate that the emission from the C719 state (peaked at  $730 \text{ nm}$ ) is significantly more intense than the emission from the C710 state, although the bulk absorption of the two states is comparable. No significant shoulder near  $710 \text{ nm}$  was observed in the bulk emission spectra (Figure 5, solid curve). These data suggest that emission from the C710 state upon high-energy (indirect) excitation is relatively weak (if present at all). On the other hand, upon direct excitation, sharp lines belonging to the C710 state were detected by Jelezko et al. in fluorescence excitation spectra even though their experimental setup, including a filter transmitting at  $\lambda > 725 \text{ nm}$ , did not favor detection of the  $\sim 710\text{--}712 \text{ nm}$  emission.<sup>30</sup> The most probable explanation for these observations involves relatively efficient energy transfer from the C710 state to the C719 state. It is noteworthy that we never observed more than two lines in a single spectrum (perhaps the result of a spectral diffusion event occurring during the collection time), while Jelezko et al.<sup>30</sup> reported up to four

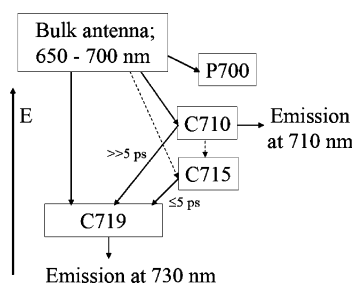


**Figure 7.** Diagram of energy-transfer processes in PS I of *Thermosynechococcus elongatus*.

lines in a single spectrum for the same collection time, 60 s. It was recently demonstrated that the red state emission is polarized,<sup>31</sup> and the differences in the number of observed lines from complex to complex in the same experiment could be explained by orientation effects. However, both in this work and in ref 30 the samples were produced in a similar manner, and it is unclear why the average orientation of the complexes should be different in this work and in ref 30. The possibility of rapid spectral diffusion (which could average away the narrow lines at long collection times) was investigated by reducing the spectrum collection time from 60 to 10, 5, and 1 s for some of the complexes that did not reveal any narrow lines. Since no narrow lines were observed even for the shortest collection times, we believe that narrow lines were truly absent in the emission spectra of some *Synechococcus* PS I complexes. It is tempting to suggest that the differences between our observations and those by Jelezko et al. are due to higher intactness of the samples used in this work, which results in a higher probability of C710  $\rightarrow$  C719 energy transfer.

The energy-transfer processes occurring in PS I of *Synechococcus* are summarized in Figure 7. The energy absorbed by the bulk antenna ( $650\text{--}700 \text{ nm}$ ) is transferred to the reaction center (P700) or to the red antenna states C710, C715, and C719. The differences from complex to complex in the relative intensities of the fluorescence originating from the C710 and C719 states may be due to orientation effects or varying probability of EET from the higher energy core states to the C710 state or to varying probability of C710  $\rightarrow$  C719 energy transfer. Unfortunately, polarization measurements employing conventional setups such as those used in this work and in refs 30 and 31 do not allow one to determine whether or not the effects related to variations in the EET probabilities are present in addition to the orientation effects. One can suggest, however, that the very fact that narrow C710 lines were observed for *Synechococcus* PS I indicates that the C710  $\rightarrow$  C719 energy-transfer times are, at least in some PS I complexes, significantly longer than 5–6 ps observed for the C706 state of *Synechocystis* by means of spectral hole burning.<sup>12</sup>

We hasten to remind the reader that while the C714 band of *Synechocystis* PCC 6803 and the C719 band of *Thermosynechococcus elongatus* very likely belong to the same chlorophyll multimer,<sup>10,12</sup> the C706 band of *Synechocystis* and the C710 band of *Synechococcus* most probably do not. It is quite possible that the C706 band of *Synechocystis* corresponds to the C715 band of *Synechococcus* since both are sensitive to the trimeric/monomeric state of the PS I complexes<sup>8,9</sup> and since no features attributable to the C715 state were observed in the single PS I spectra of *Synechococcus* as well as for the C706 state in *Synechocystis*. The latter observation suggests that the C715  $\rightarrow$  C719 energy transfer in *Synechococcus* occurs on a time scale of  $\leq 5 \text{ ps}$  (as for C706  $\rightarrow$  C714 energy transfer in *Synechocystis*), in agreement with assignment of the C715 and C719 (or C706



and C714) states to two chlorophyll multimers located close to each other in the trimerization domain, i.e., B37–B38 and B7–A32. (In SHB experiments<sup>12</sup> zero-phonon holes could be observed even if energy transfer is very fast because the spectra are accumulated.) However, it cannot be excluded that fast spectral diffusion, in addition to fast energy transfer, contributes to our inability to observe narrow lines originating from the C706 state of *Synechocystis* and the C715 state of *Thermosynechococcus elongatus*.

## Conclusions

It has been demonstrated that combining spectral hole-burning and single-complex spectroscopies (using the same PS I preparations) provides unique insights into the excitonic structure and excitation energy-transfer processes in these complex biological systems. Application of both bulk and single-entity techniques is especially informative when the spectroscopic properties of the systems under study are dependent on sample preparation. We used highly purified PS I crystals from *Thermosynechococcus elongatus* similar to those used in X-ray diffraction experiments; dissolved crystals yielded samples whose absorption spectra revealed significantly stronger “red” antenna bands. These samples have also provided more convincing data that PS I from *Thermosynechococcus elongatus* indeed possesses three “red” antenna states, i.e., C710, C715, and C719, in agreement with our earlier assignment.<sup>10</sup> In addition, the presence of the narrow ZPLs in the vicinity of 710 nm in the emission spectra of single PS I complexes from *Thermosynechococcus elongatus* has been confirmed. Their weakness suggests that the energy transfer from the C710 to the C719 state is relatively efficient. The absence of narrow lines near 706–708 nm in the emission spectra of single PS I complexes from *Synechocystis* PCC 6803 indicates that energy transfer from the C706 state to the C714 state is fast (~5 ps) and efficient. Finally, our results provide additional proof of the similarity of the lowest energy states of PS I from *Synechococcus* and *Synechocystis* (C719 and C714, respectively) as well as of the presence of two different red antenna bands (C706 and C714) in PS I of *Synechocystis* PCC 6803.

**Acknowledgment.** We acknowledge Dr. John M. Hayes (Ames Laboratory USDOE) and Mr. Tse-Ming Hsin (ISU) for their involvement in the early stages of the project and Drs. Ingo Grotjohann and Hongqi Yu (ASU) for their participation in preparation of *Thermosynechococcus elongatus* PS I crystals. We thank Dr. Fedor Jelezko (University of Stuttgart) for sharing unpublished details of his experiments on *Thermosynechococcus elongatus*.

## References and Notes

- (1) Fromme, P.; Mathis, P. *Photosynth. Res.* **2004**, *80*, 109.
- (2) Jordan, P.; Fromme, P.; Witt, H. T.; Klukas, O.; Saenger, W.; Krauss, N. *Nature* **2001**, *411*, 909.
- (3) Ben-Shem, A.; Frolov, F.; Nelson, N. *Nature* **2003**, *426*, 630.
- (4) Jolley, C.; Ben-Shem, A.; Nelson, N.; Fromme, P. *J. Biol. Chem.* **2005**, *280*, 33627.
- (5) Bibby, T. S.; Nield, J.; Partensky, F.; Barber, J. *Nature* **2001**, *413*, 590.
- (6) Bibby, T. S.; Nield, J.; Barber, J. *Nature* **2001**, *412*, 743.
- (7) Boekma, E. J.; Hifney, A.; Yakushevskaya, A. E.; Piotrowsky, M.; Keegstra, W.; Berry, S.; Michel, K.-P.; Pistorius, E. K.; Kruip, J. *Nature* **2001**, *412*, 745.
- (8) Pålsson, L.-O.; Dekker, J. P.; Schlodder, E.; Monshouwer, R. van Grondelle, R. *Photosynth. Res.* **1996**, *48*, 239.
- (9) Rätsep, M.; Johnson, T. W.; Chitnis, P. R.; Small, G. J. *J. Phys. Chem. B* **2000**, *104*, 836.
- (10) Zazubovich, V.; Matsuzaki, S.; Johnson, T. W.; Hayes, J. M.; Chitnis, P. R.; Small, G. J. *Chem. Phys.* **2002**, *275*, 47.
- (11) Melkozernov, A. N.; Lin, S.; Blankenship, R. E.; Valkunas, L. *Biophys. J.* **2001**, *81*, 1144.
- (12) Hsin, T.-M.; Zazubovich, V.; Hayes, J. M.; Small, G. J. *J. Phys. Chem. B* **2004**, *108*, 10515.
- (13) Byrdin, M.; Jordan, P.; Krauss, N.; Fromme, P.; Stehlik, D.; Schlodder, E. *Biophys. J.* **2002**, *83*, 433.
- (14) Sener, M. K.; Lu, D.; Ritz, T.; Park, S.; Fromme, P.; Schulten, K. *J. Phys. Chem. B* **2002**, *106*, 7948.
- (15) Damjanovic, A.; Vaswani, H. M.; Fromme, P.; Fleming, G. R. *J. Phys. Chem. B* **2002**, *106*, 10251.
- (16) Balaban, T. S. *FEBS Lett.* **2003**, *545*, 97. Erratum *FEBS Lett.* **2003**, *547*, 235.
- (17) Balaban, T. S. Private communication.
- (18) Gobets, B.; van Stokkum, I. H. M.; van Mourik, F.; Dekker, J. P.; van Grondelle, R. *Biophys. J.* **2003**, *85*, 3883.
- (19) Köhler, M.; Friedrich, J.; Fidy, J. *Biochem. Biophys. Acta* **1998**, *1386*, 255.
- (20) Hofman, C.; Ketelaars, M.; Matsushita, M.; Michel, H.; Aartsma, T.; Köhler, J. *Phys. Rev. Lett.* **2003**, *90*, 13004.
- (21) Hofman, C.; Aartsma, T.; Michel, H.; Köhler, J. *Proc. Natl. Acad. Sci. U.S.A.* **2003**, *100*, 15534.
- (22) Ketelaars, M.; Matsushita, M.; van Oijen, A. M.; Köhler, J.; Aartsma, T. J.; Schmidt, J. *Biophys. J.* **2001**, *80*, 1591.
- (23) Matsushita, M.; Ketelaars, M.; van Oijen, A. M.; Köhler, J.; Aartsma, T. J.; Schmidt, J. *Biophys. J.* **2001**, *80*, 1604.
- (24) Tietz, C.; Chekhlov, O.; Dräbenstedt, A.; Schuster, J.; Wrachtrup, J. *J. Phys. Chem. B* **1999**, *103*, 6328.
- (25) van Oijen, A. M.; Ketelaars, M.; Köhler, J.; Aartsma, T. J.; Schmidt, J. *Chem. Phys.* **1999**, *247*, 53.
- (26) van Oijen, A. M.; Ketelaars, M.; Köhler, J.; Aartsma, T. J.; Schmidt, J. *Biophys. J.* **2000**, *78*, 1570.
- (27) Gerken, U.; Jelezko, F.; Götze, B.; Branschädel, M.; Tietz, C.; Ghosh, R.; Wrachtrup, J. *J. Phys. Chem. B* **2003**, *107*, 338.
- (28) Ketelaars, M.; Hoffman, C.; Köhler, J.; Howard, T. D.; Cogdell, R. J.; Schmidt, J.; Aartsma, T. J. *Biophys. J.* **2002**, *83*, 1701.
- (29) Tietz, C.; Jelezko, F.; Gerken, U.; Schuler, S.; Schubert, A.; Rogl, H.; Wrachtrup, J. *Biophys. J.* **2001**, *81*, 556.
- (30) Jelezko, F.; Tietz, C.; Gerken, U.; Wrachtrup, J.; Bittl, R. *J. Phys. Chem. B* **2000**, *104*, 8093.
- (31) Elli, A. F.; Jelezko, F.; Tietz, C.; Studier, H.; Brecht, M.; Bittl, R.; Wrachtrup, J. *Biochemistry* **2006**, *45*, 1454.
- (32) Pålsson, L.-O.; Fleming, C.; Gobets, B.; van Grondelle, R.; Dekker, J.; Schlodder, E. *Biophys. J.* **1998**, *74*, 2611.
- (33) Gobets, B.; van Amerongen, H.; Monshouwer, R.; Kruip, J.; Rögner, M.; van Grondelle, R.; Dekker, J. P. *Biochem. Biophys. Acta* **1994**, *1188*, 75.
- (34) Hayes, J. M.; Matsuzaki, S.; Rätsep, M.; Small, G. J. *J. Phys. Chem. B* **2000**, *104*, 5625.